Available online at www.sciencedirect.com

ScienceDirect

Energy Procedia 124 (2017) 188–196

Energy Procedia

www.elsevier.com/locate/procedia

7th International Conference on Silicon Photovoltaics, SiliconPV 2017

Effect of low-temperature annealing on defect causing copper-related light-induced degradation in p-type silicon

Henri Vahlman[a,*], Antti Haarahiltunen[a], Wolfram Kwapil[b], Jonas Schön[b], Marko Yli-Koski[a], Alessandro Inglese[a], Chiara Modanese[a], Hele Savin[a]

[a]*Department of Electronics and Nanoengineering, Aalto University, Tietotie 3, 02150 Espoo, Finland*
[b]*Fraunhofer Institute for Solar Energy Systems ISE, Heidenhofstr. 2, 79110 Freiburg, Germany*

Abstract

Copper is a common impurity in photovoltaic silicon. While reported to precipitate instantly in n-type Si, copper causes light-induced degradation (Cu-LID) in p-type Si. Recently, partial recovery of Cu-LID was observed after only few minutes of dark annealing at 200 °C. In this contribution, we investigate the effects of the dark anneal on Cu-LID-limited minority carrier lifetime both experimentally and by simulations. Surprisingly, after initial recovery, the dark anneal results in further degradation corresponding to a many-fold increase in recombination activity compared to the degraded state after illumination. This anneal-induced degradation can potentially cause additional losses in accidentally Cu-contaminated devices when exposed to elevated temperatures, for example during recovery and regeneration treatments of solar cells. Transient ion drift measurements confirmed that the anneal-induced degradation cannot be attributed to residual interstitial Cu after illumination. After hundreds of hours of annealing, the samples showed another recovery. To analyze these experimental results, a comparison to simulations is performed at the end of the paper.

Peer review by the scientific conference committee of SiliconPV 2017 under responsibility of PSE AG.

Keywords: silicon; LID; Cu; recovery; precipitate

1. Background

Due to its high diffusivity in silicon, copper can be introduced into photovoltaic Si for example from ingot growth, wafer dicing, contaminated manufacturing equipment, or from Cu contacts and interconnects [1, 2]. Cu concentrations between 10^{13} cm^{-3} and 10^{15} cm^{-3} are typically measured in as-grown multicrystalline silicon (mc-Si) wafers [3-7]. The fast diffusivity of Cu promotes its response to gettering treatments, and Cu levels below detection limits of available analytical methods [e.g. inductively coupled plasma mass spectrometry (ICP-MS)] after

1876-6102
Peer review by the scientific conference committee of SiliconPV 2017 under responsibility of PSE AG.
10.1016/j.egypro.2017.09.314

phosphorus diffusion gettering (PDG) have been reported by different groups [4, 8]. However, the gettering efficiency during solar cell fabrication depends on the cell architecture and process details, and reduced response to gettering has been reported in heavily defected materials [9, 10]. In addition, Cu has been found to limit solar cell efficiency even in concentrations below the detection limit of ICP-MS (i.e. $<10^{13}$ cm^{-3}) [11]. The Cu impurity causes light-induced degradation (Cu-LID) in p-type Si, which has been found in mc-Si material both on wafer [12-15] and solar cell [16-18] level. Although grain boundaries of mc-Si are considered effective gettering sinks for transition metals, significant Cu-LID occurs also in the intra-grain areas of as-grown p-type mc-Si [15]. Recently, considerable Cu-LID resulting in efficiency degradation of several $\%_{rel}$ was detected in industrially manufactured PERC-type solar cells made from seed-cast quasi-monocrystalline silicon, which means that emitter formation does not necessarily result in sufficient Cu removal from the base [18]. Hence, Cu-LID is a potential source of efficiency loss in industrial high-efficiency solar cells.

Recently, the Cu-LID defect was identified to be likely a precipitate through temperature- and injection-dependent lifetime spectroscopy [19]. Subsequently, we have developed a model for Cu-LID as precipitation of interstitial Cu_i^+ [20]. The model is based on calculating the growth of positively charged, spherically shaped metallic Cu_3Si precipitates using chemical rate equations, where growth and dissolution rates of the precipitates were modified to take into account the electrostatic repulsion between the Cu_i^+ cations and the charged precipitates. The recombination activity of the precipitates is calculated based on the thermionic emission theory based on a previously published Schottky junction model [21, 22]. This approach allowed simulating Cu-LID on minority carrier lifetime level, and provided evidence for the theory of Cu-LID as a precipitate formation process [23]. Further support was obtained in Ref. [24], where the experimental injection-dependent minority carrier lifetime after Cu-LID was fitted by varying the free parameters of the parametrization presented in Ref. [22] that is based on the above-mentioned Schottky junction model. Thus, considering the current evidence, the most likely explanation for Cu-LID is precipitate formation during illumination.

Recovery and regeneration of LID causing defects such as the well-known boron-oxygen (BO) defect and the light- and elevated temperature-induced degradation (LeTID) often involve heating the solar cells or test substrates up to above 200 °C [25-27]. Since it is possible that also other lifetime-limiting defects, such as the Cu impurity, are present [18], it is relevant to gain more understanding also on the behavior of these other mechanisms during the annealing treatments. Recently, partial recovery of Cu-LID was observed in the same conditions and timescale [28] as for the well-known boron-oxygen (BO) defect, which recovers fully after dark annealing at 200 °C for 2-10 min [29]. In Ref. [28], a diffusion length recovery from 60 to 100 µm was experimentally observed after a few min anneal at 200 °C in 1 Ωcm float-zone (FZ) Si with a Cu contamination level of 1×10^{14} cm^{-3}. In this contribution, we further investigate the effects of dark annealing, and whether our Cu-LID model can provide physical insight into the mechanism that apparently enables the lifetime recovery of the Cu-LID defect at as low as 200 °C.

2. Experimental details

Experiments were performed with 400 µm thick Czochralski (Cz) and 250 µm thick FZ Si wafers with resistivity of 3.6 Ωcm and 1 Ωcm, respectively. The samples were thermally oxidized at 900 °C in O_2 for 40 min, followed by a 20 min anneal in N_2. Cu contamination was performed with the spin-on method, resulting in approximate bulk Cu_i^+ concentrations of 5×10^{13}–1×10^{14} cm^{-3} after in-diffusion at 800 °C in N_2, depending on the concentration of the contamination solution and the wafer thickness [30].

After a +600 nC cm^{-2} corona charge deposition on both wafer surfaces, the samples were degraded under 0.65 sun illumination at room temperature (RT) while lifetime was recorded with the quasi-steady-state photoconductance decay method (Sinton Instruments). Annealing was performed either on a hotplate or in a furnace. To compensate for surface charge lost during annealing, corona charge was added after each anneal until the effective lifetime saturated.

Interstitial Cu concentration was measured with the transient ion drift (TID) method [31]. The TID method is based on measuring changes in the capacitance of a Schottky diode, which derives from the drift of mobile ions away from the depletion region when a reverse bias voltage is applied. The change in the junction capacitance, ΔC,

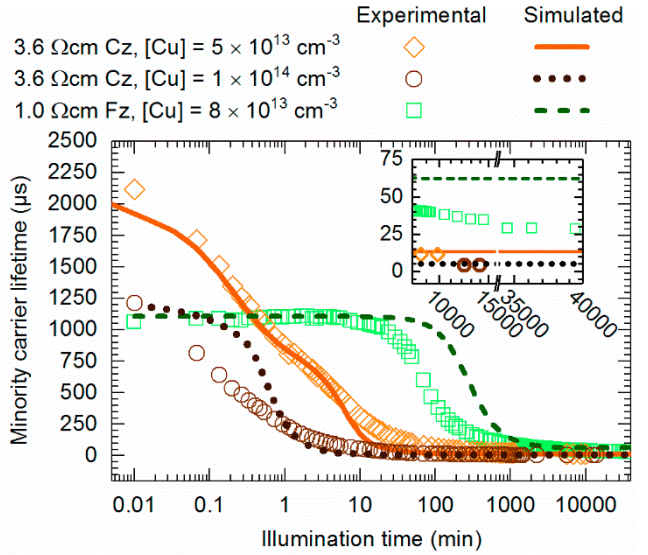

Fig. 1. Experimental and simulated minority carrier lifetime degradation of two 3.6 Ωcm Cz samples and a 1 Ωcm FZ sample, contaminated with [Cu] = 5×10^{13} cm^{-3}, [Cu] = 1×10^{14} cm^{-3}, and 8×10^{13} cm^{-3}, respectively. The lifetime is determined at the excess carrier concentration of Δn = 0.1 times the doping level.

has been shown to be approximately proportional to the average concentration of mobile ions in the bulk [31]. The TID sample preparation involved removing the surface oxide using hydrofluoric acid, followed by a piranha etch [a mixture of H_2SO_4 (96 % vol/vol) and H_2O_2 (30 % vol/vol) in 4:1 volume ratio, respectively] for 13 sec. A Schottky contact was formed on the front side of the wafer by evaporating a thin Al film, whereas an ohmic contact was formed on the backside with InGa paste.

Density of interface traps (D_{it}) is a quantity that is directly proportional to the recombination velocity at the wafer surface [32]. The D_{it} was measured using the contactless corona voltage (C-V) method using a PV-2000 tool [33].

3. Results and discussion

3.1. Light-induced degradation

Experimental Cu-LID data is compared in Fig. 1 with simulated minority carrier lifetime which is calculated according to the model presented in Ref. [20], combining precipitation simulations with the calculation of the minority carrier lifetime based on the thermionic emission theory. The reader is referred to Ref. [20] for full details of the calculation of the precipitate growth and the recombination activity. Note that in the case of 3.6 Ωcm Cz, the first few minutes are dominated by the FRC stage of the BO defect, whereas the final part is limited by Cu precipitates as described in [23]. With the present batch of samples, the best agreement between simulations and experiments was obtained by setting the term corresponding to the surface energy between the Cu_3Si precipitates and the Si lattice to $\gamma = 5.9 \times 10^{-5}$ J cm^{-2}, which deviates from the originally used fitted value of $\gamma = 6.15 \times 10^{-5}$ J cm^{-2} in [23] most likely due to fluctuations in the in-diffused [Cu]. Other energetic and kinetic parameters, that is, the free energy change per precipitate volume due to strain and the chemical reaction rate at the precipitate–Si interface, were held at the same values as in [23]. The experimental LID behavior is qualitatively reproduced with these fitted values in case of different doping and Cu concentrations. In 3.6 Ωcm Cz with [Cu] = 5×10^{13} cm^{-3}, the simulated final lifetime is 13 µs (very close to 11 µs of the experiments). The final precipitate radius and density distributions after LID are illustrated in Fig. 2, where, in the case of the mentioned sample with [Cu] = 5×10^{13} cm^{-3}, the average precipitate radius and density are 2.3 nm and 1.4×10^{10} cm^{-3}, respectively. Increasing [Cu] to 1×10^{14} cm^{-3} results in a decrease in both experimental and simulated final lifetime (6.2 µs and 5.1 µs, respectively), which

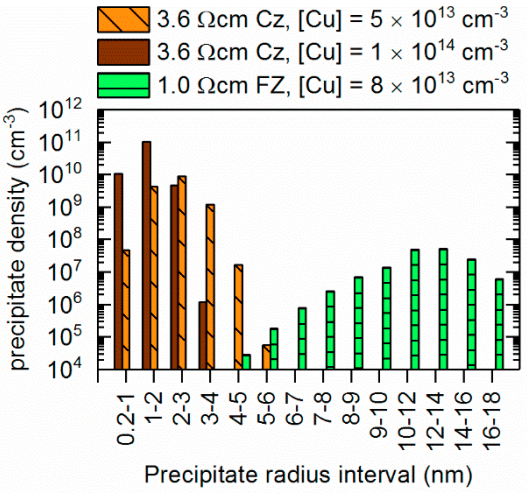

Fig. 2. Simulated precipitate radius and density distribution after LID.

according to the simulations stems from a decrease in the radius (1.4 nm) and an increase in the density (1.2×10^{11} cm^{-3}) of precipitates. In the case of the 1 Ωcm FZ sample (no BO defect) with [Cu] = 8×10^{13} cm^{-3}, the simulations result in a higher final lifetime (62 µs) than the experiments (28 µs), with simulated precipitate radius and density of 12 nm and 1.6×10^{8} cm^{-3}, respectively. The notable difference in the simulated precipitate size and density between 3.6 Ωcm and 1 Ωcm samples derives from the solubility of Cu increasing with the doping concentration, which lowers the level of supersaturation in the 1 Ωcm material in comparison to the 3.6 Ωcm material at similar impurity densities [23].

3.2. Effect of annealing on experimentally measured lifetime

Fig. 3 shows the results of a recovery anneal at 200 °C that was performed on the sample types of Fig. 1 after illumination and saturation of the minority carrier lifetime. In the 1 Ωcm FZ sample, a qualitatively similar early recovery from 28 µs to 43 µs as in Ref. [28] is experimentally observed during the first few minutes. However, unexpectedly, after few minutes the recovery turns into considerable degradation. In the case of the two 3.6 Ωcm Cz samples with [Cu] = 5×10^{13} cm^{-3} of Fig. 3, the other one shows a slight early recovery while the other did not recover at all. Nevertheless, both of these samples exhibit a similar collapse-like degradation as the FZ sample, which in this case occurs after a widely varying interval between 1 and 1000 mins of annealing. This behavior was also observed in a similar Cz sample illuminated as long as 3.5 months at 75 °C prior to the annealing treatment (data not shown). Qualitatively similar phenomena were seen also in the 3.6 Ωcm Cz sample with [Cu] = 1×10^{14} cm^{-3}, although to a lesser extent. Based on the presented results, in spite of the initial lifetime recovery, the most visible effect of the annealing treatment in most samples is a further degradation of the lifetime. The degradation observed in Fig. 3 corresponds to up to six-fold increase in the total recombination activity. This increase is not attributable to other metastable defects, that is, the boron-oxygen defect and the dissociation of iron-boron pairs (FeB) to interstitial iron (Fe_i), since these mechanisms are expected to increase the effective lifetime at the investigated temperature and injection-level range (i.e. >200 °C and $\Delta n > 3 \times 10^{14}$ cm^{-3}, respectively) [25, 34]. It is noteworthy that in addition to the annealing-induced degradation, the samples of Fig. 3 also show a very slow recovery tendency upon prolonged annealing (illustrated with an inset), which is investigated further in Sec. 3.3.

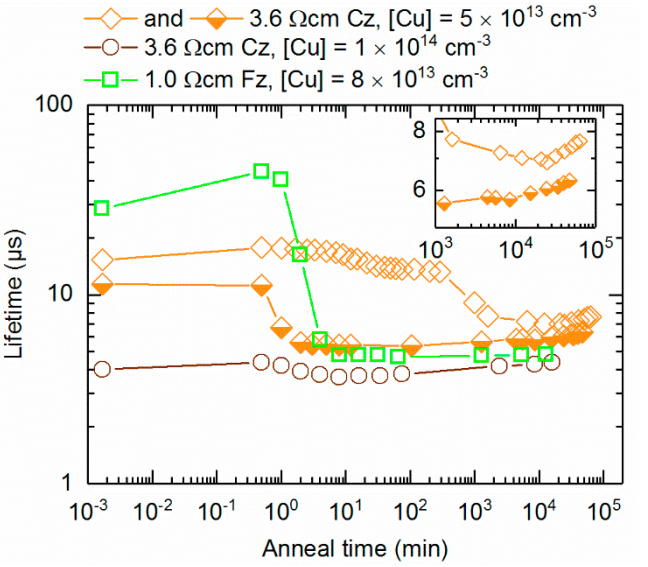

Fig. 3. Experimental minority carrier lifetime (at Δn = 0.1 × doping level) in Cz and FZ wafers during dark annealing at 200 °C. The inset is a zoom showing the slow recovery of the Cz samples with [Cu] = 5 × 10^{13} cm^{-3} during long annealing times from 10^3 to 10^5 min.

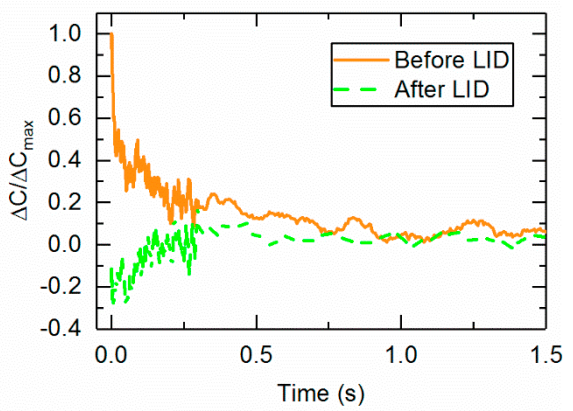

Fig. 4. Normalized transient capacitance signal during a reverse voltage pulse before and after LID in samples contaminated with [Cu] = 5 × 10^{13} cm^{-3}. ΔC is the change in the capacitance during the reverse voltage pulse, and the normalization is done against ΔC_{max}, corresponding to the maximum value of ΔC in the "Before LID"-sample.

In order to study if the above-described annealing-induced lifetime degradation could derive from non-precipitated interstitial Cu that would still reside in the interstitial state despite thousands of minutes or even several months of illumination, transient ion drift (TID) measurements were performed using Cz samples with [Cu] = 5 × 10^{13} cm^{-3}. Fig. 4 shows the change in the capacitance signal, $\Delta C = C(t) - C(t \to \infty)$, both before and after LID, which is normalized against the maximum value of ΔC [i.e. $\Delta C_{max} = C(0) - C(t \to \infty)$] as measured before LID. A clear capacitance change is visible before LID. This change was in the positive direction, that is, the total capacitance increased when the reverse bias voltage was applied, which is consistent with the behavior earlier reported for Cu_i^+ [35]. Here we note that the quantity $\Delta C/\Delta C_{max}$ was observed to decrease in the "Before LID"-sample with storage time due to Cu_i^+ out-diffusion to the wafer surface (data not shown) [36]. On the other hand, degraded samples (after LID but before annealing) showed no change of capacitance signal that could be interpreted

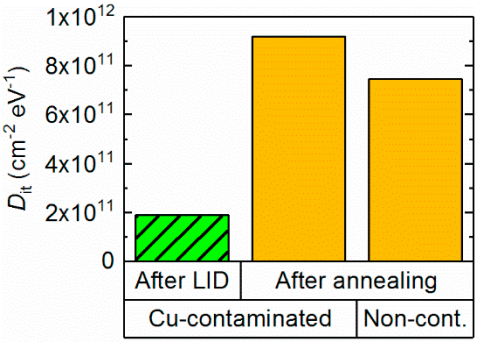

Fig. 5. Density of interface traps (D_{it}) in Cu-contaminated samples ([Cu] = 5 × 10^{13} cm^{-3}) both after LID and after annealing, and in a reference non-contaminated sample after annealing. The annealing step increases D_{it} approximately similarly both in the Cu-contaminated and the non-contaminated samples.

to derive from residual Cu_i^+. The origin of the slight negative shift in the beginning of the "After LID" TID signal (indicating a ΔC opposite in sign to ΔC_{max} of the "Before LID"-sample against which the data was normalized) is unclear but cannot be attributed to mobile positively charged ionic species [35]. Therefore, the further degradation during annealing most likely derives from other effects than residual Cu_i^+.

As no residual Cu_i^+ was found in the wafers after LID, the next step was to study if the degradation upon annealing derives from degradation of the surface oxide. Hence, a non-contaminated reference wafer (1 Ωcm FZ) was surface passivated and annealed similarly to the Cu-contaminated wafers in Fig. 3. Although some degradation was observed also in the reference wafer upon annealing, the lifetime remained above 250 µs throughout the annealing treatment, and the strong degradation of the Cu-contaminated wafers was absent. To investigate whether the surface of the Cu-contaminated samples could degrade more than that of the reference wafer (due to e.g. surface precipitation of Cu), density of interface traps (D_{it}) was measured in both cases. The results, shown in Fig. 5, indicate a similar increase in D_{it} after annealing both in the Cu-contaminated wafers (an average over two wafers with [Cu] = 5 × 10^{13} cm^{-3} and three measurement points) and the non-contaminated reference wafer (average over six measurement points). Hence, although the annealing treatment seems to degrade the surface passivation somewhat, it cannot be attributed to Cu-related effects. This means that surface passivation degradation during annealing does not explain the observed collapse in the lifetime of the Cu-contaminated samples in Fig. 3.

3.3. Comparison between experiments and simulations

Since the Cu-LID model presented in Ref. [20] was observed to reproduce the experimental Cu-LID-limited lifetimes well both in Ref. [23] and Fig. 1, it is relevant to compare experiments and simulations also in the case of the prolonged dark annealing treatment at 200 °C studied in this paper. The annealing behavior was simulated using the simulated final precipitate size and density distribution after LID in Fig. 2 as an initial condition, and using the above-fitted value of the interface energy, γ = 5.9 × 10^{-5} J cm^{-2}, as the energetic parameter (affecting the effective solubility) whose adjustment is necessary to reach compliance between LID experiments and the simulations (see Refs. [20] and [23]). We note here that the dark annealing simulation predicts neither the early recovery after few minutes, observed in part of the samples in Fig. 3 and in Ref. [28], nor the annealing-induced degradation. This means that these phenomena are not explainable with simple precipitate growth and dissolution that the model presented in [20] is based upon. Therefore, the degradation during annealing may be related to changes in the properties of the precipitates that the model does not consider, such as a morphology change of the precipitates or changes in precipitate–Si interface properties. Another alternative is that the annealing causes an increase in the bulk recombination activity that is not directly related to the precipitates. For example, dissociation of a complex composed of four Cu atoms has been reported upon annealing of Cu-contaminated Si at >150 °C, possibly resulting in the formation of recombination active substitutional Cu [37, 38].

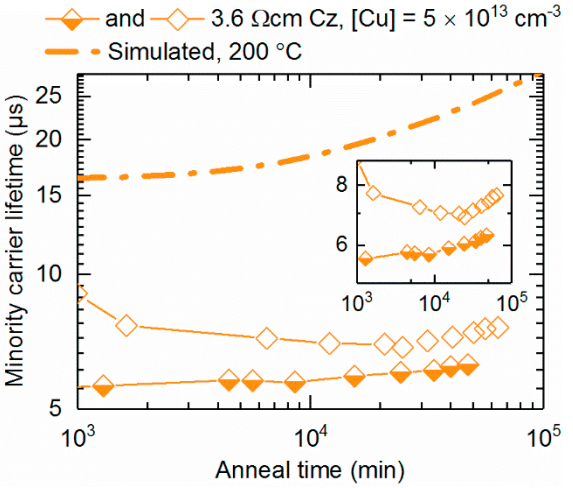

Fig. 6. Simulated minority carrier lifetime (at Δn = 0.1 × doping level) in 3.6 Ωcm Cz with [Cu] = 5 × 10^{13} cm^{-3} as compared to experiments (the same samples as in Fig. 3) during annealing at 200 °C. The inset is a zoom to 5–9 µs.

Although the simulation of the dark anneal reproduces neither the early recovery nor the anneal-induced degradation, a long-term recovery trend emerges after several thousand minutes, which shows qualitative resemblance to the long-term recovery stage of the experiments. This is illustrated in Fig. 6 showing the final part of both the simulated and the experimental annealing treatment at 200 °C in the case of the 3.6 Ωcm Cz samples of Fig. 3 with [Cu] = 5 × 10^{13} cm^{-3}. Although the simulation clearly overestimates the extent of the long-term recovery in comparison to the experiments, it may give physical insight into the root cause of this phenomenon. The simulated lifetime recovery follows from annealing-induced precipitate growth that increases the average precipitate size and simultaneously decreases the precipitate density. According to the model [20], the simulated precipitate growth follows from a five orders of magnitude increase in Cu solubility when the temperature increases from RT to 200 °C. This increase will start dissolving all precipitate sizes, which increases the concentration of interstitial Cu in the Si lattice slightly. When the reintroduced interstitial Cu has increased the level of supersaturation sufficiently, large precipitate sizes will start to grow again (while the small ones continue dissolving) because the energetic cost of adding single Cu atoms into large precipitates is lower than their incorporation into small precipitates due to a smaller increase of stress and surface energy per included Cu atom. The simulated precipitate growth results in a decrease in the total precipitate–Si interface area in the silicon bulk and consequently the total recombination activity of the precipitates diminishes, which leads to the simulated lifetime recovery. With these considerations, the overestimation of the simulated recovery in comparison to experiments may be related for example to overestimation of the increase in the Cu solubility upon the mentioned temperature increase from RT to 200 °C (experimental solubility data only exists at >500 °C [39], which was extrapolated to lower temperatures in the simulations [20]).

4. Conclusions

The behavior of the Cu-LID defect during low-temperature dark annealing was studied. Unexpectedly, although a brief initial recovery occurred in part of the samples, a further degradation after few minutes to several hundred minutes of annealing at 200 °C occurred, which resulted in up to six-fold increase in the total recombination activity. This may cause significant further degradation in Cu-contaminated devices if subjected to elevated temperatures, such as during recovery or regeneration treatments of solar cells. Although this further degradation raises a question whether all interstitial Cu has precipitated during the preceding illumination stage, no Cu_i^+ was detected with TID measurements after illumination. Based on D_{it} measurements and reference samples, the anneal-

induced degradation seems to be related to the properties of the bulk Cu-LID defect itself or other bulk phenomena instead of changes in the wafer surface passivation. According to simulations, it was not possible to explain either the early recovery effect after few minutes of annealing or the further annealing-induced degradation stage with precipitate dissolution or growth. Hence, either the anneal at 200 °C causes changes in the precipitate morphology or interface properties that the model does not take into account, or the mentioned phenomena are caused by other currently unidentified bulk defects. A long-term recovery stage emerged during prolonged annealing, which based on simulations was speculated to derive from annealing-induced precipitate growth. Observation of the Cu-LID defect with microscopy methods, which has not been achieved at present and is made challenging by the probable small (nanometer-scale) size of the precipitates [23, 24], might provide further insights into the interpretation of the presented results.

Acknowledgements

The work has been funded through the European Research Council under the European Union's FP7 Programme ERC Grant Agreement No. 307315. A.I. acknowledges the financial support of Aalto ELEC doctoral school and Alfred Kordelin Foundation.

References

[1] Istratov AA, Weber ER. Physics of copper in silicon. *J Electrochem Soc* 2002;149:G21-G30.
[2] Kraft A, Wolf C, Bartsch J, Glatthaar M, Glunz S. Long term stability of copper front side contacts for crystalline silicon solar cells. *Sol Energ Mat Sol Cells* 2015;136:25-31.
[3] Istratov AA, Buonassisi T, McDonald RJ, Smith AR, Schindler R, Rand JA, Kalejs JP, Weber ER. Metal content of multicrystalline silicon for solar cells and its impact on minority carrier diffusion length. *J Appl Phys* 2003;94:6552-6559.
[4] Morishige AE, Jensen MA, Hofstetter J, Yen PXT, Wang C, Lai B, Fenning DP, Buonassisi T. Synchrotron-based investigation of transition-metal getterability in n-type multicrystalline silicon. *Appl Phys Lett* 2016;108:202104.
[5] Bredemeier D, Walter D, Herlufsen S, Schmidt J. Lifetime degradation and regeneration in multicrystalline silicon under illumination at elevated temperature. *AIP Adv* 2016;6:035119.
[6] Riepe S, Reis IE, Kwapil W, Falkenberg MA, Schön J, Behnken H, Bauer J, Kreßner-Kiel D, Seifert W, Koch W. Research on efficiency limiting defects and defect engineering in silicon solar cells - results of the German research cluster SolarFocus. *Phys Status Solidi C* 2011;8:733-738.
[7] Schön J, Schindler F, Kwapil W, Knörlein M, Krenckel P, Riepe S, Warta W, Schubert MC. Identification of the most relevant metal impurities in mc n-type silicon for solar cells. *Sol Energ Mat Sol Cells* 2015:142:107-115.
[8] Shabani MB, Yamashita T, Morita E. Metallic Impurities in Mono and Multi-crystalline Silicon and Their Gettering by Phosphorus Diffusion. *ECS Transactions* 2008;16:179-193.
[9] Bentzen A, Holt A, Kopecek R, Stokkan G, Christensen JS, Svensson BG. Gettering of transition metal impurities during phosphorus emitter diffusion in multicrystalline silicon solar cell processing. *J Appl Phys* 2006;99:093509.
[10] Castellanos S, Ekstrom KE, Autruffe A, Jensen MA, Morishige AE, Hofstetter J, Yen P, Lai B, Stokkan G, Del Canizo C, Buonassisi T. High-performance and traditional multicrystalline silicon: Comparing gettering responses and lifetime-limiting defects. *IEEE J Photovolt* 2016;6:632-640.
[11] Bertoni MI, Fenning DP, Rinio M, Rose V, Holt M, Maser J, Buonassisi T. Nanoprobe X-ray fluorescence characterization of defects in large-area solar cells. *Energy Environ Sci* 2011;4:4252-4257.
[12] Tarasov I, Ostapenko O. *Eighth Workshop on Crystalline Silicon Solar Cell Materials and Processes,* Copper Mountain, Colorado, USA, 17-19 August 1998, (NREL, Golden, CO, USA, 1998), p. 207-210.
[13] Savin H, Yli-Koski M, Haarahiltunen A. Role of copper in light induced minority-carrier lifetime degradation of silicon. *Appl Phys Lett* 2009;95:152111.
[14] Lindroos J, Savin H. Formation kinetics of copper-related light-induced degradation in crystalline silicon. *J Appl Phys* 2014;116:234901.
[15] Lindroos J, Boulfrad Y, Yli-Koski M, Savin H. Preventing light-induced degradation in multicrystalline silicon. *J Appl Phys* 2014;115:154902.
[16] Turmagambetov T, Dubois S, Garandet JP, Martel B, Enjalbert N, Veirman J, Pihan E. Influence of copper contamination on the illuminated forward and dark reverse current-voltage characteristics of multicrystalline p-type silicon solar cells. *Phys Status Solidi C* 2014;11:1697-1702.
[17] Luka T, Turek M, Großer S, Hagendorf C. Microstructural identification of Cu in solar cells sensitive to light-induced degradation. *Phys Status Solidi RRL* 2017;11:1600426.
[18] Vahlman H, Wagner M, Wolny F, Krause A, Laine H, Inglese A, Yli-Koski M, Savin H. Light-induced degradation in quasi-monocrystalline silicon PERC solar cells: Indications on involvement of copper. *Phys Status Solidi A* 2017;e201700321.
[19] Inglese A, Lindroos J, Vahlman H, Savin H. Recombination activity of light-activated copper defects in p-type silicon studied by injection- and temperature-dependent lifetime spectroscopy. *J Appl Phys* 2016;120:125703.

[20] Vahlman H, Haarahiltunen A, Kwapil W, Schön J, Inglese A, Savin H. Modeling of light-induced degradation due to Cu precipitation in p-type silicon. I. General theory of precipitation under carrier injection. *J Appl Phys* 2017;121:195703.
[21] Plekhanov PS, Tan TY. Schottky effect model of electrical activity of metallic precipitates in silicon. *Appl Phys Lett* 2000;76:3777-3779.
[22] Kwapil W, Schön J, Warta W, Schubert MC. Carrier Recombination at Metallic Precipitates in p-and n-Type Silicon. *IEEE J Photovolt* 2015;5:1285-1292.
[23] Vahlman H, Haarahiltunen A, Kwapil W, Schön J, Inglese A, Savin H. Modeling of light-induced degradation due to Cu precipitation in p-type silicon. II. Comparison of simulations and experiments. *J Appl Phys* 2017;121:195704.
[24] Inglese A, Vahlman H, Kwapil W, Schön J, Savin H. Characterization of light-activated Cu defects in silicon: Comparison with the recombination activity of metallic precipitates. *Phys Status Solidi C* 2017;1700103.
[25] Schmidt J, Bothe K. Structure and transformation of the metastable boron- and oxygen-related defect center in crystalline silicon. *Phys Rev B* 2004;69:241071-241078.
[26] Herguth A, Schubert G, Kaes M, Hahn G. *Conference Record of the 2006 IEEE 4th World Conference on Photovoltaic Energy Conversion, WCPEC-4,* Waikoloa, Hawaii, USA, 2006, (IEEE, New York, 2007), p. 940-943.
[27] Payne DNR, Chan CE, Hallam BJ, Hoex B, Abbott MD, Wenham SR, Bagnall DM. Acceleration and mitigation of carrier-induced degradation in p-type multi-crystalline silicon. *Phys Status Solidi RRL* 2016;10:237-241.
[28] Inglese A, Lindroos J, Savin H. Accelerated light-induced degradation for detecting copper contamination in p -type silicon. *Appl Phys Lett* 2015;107:052101.
[29] Schmidt J, Aberle AG, Hezel R. *Conference Record of the Twenty Sixth IEEE Photovoltaic Specialists Conference - 1997,* Anaheim, California, USA, 29 September-3 October 1997, (IEEE, New York, 1997), p. 13-18.
[30] Väinölä H, Saarnilehto E, Yli-Koski M, Haarahiltunen A, Sinkkonen J, Berenyi G, Pavelka T. Quantitative copper measurement in oxidized p-type silicon wafers using microwave photoconductivity decay. *Appl Phys Lett* 2005;87:032109.
[31] Heiser T, McHugo S, Hieslmair H, Weber ER. Transient ion drift detection of low level copper contamination in silicon. *Appl Phys Lett* 1997;70:3576-3578.
[32] Fitzgerald DJ, Grove AS. Surface recombination in semiconductors. *Surface Science* 1968;9:347-369.
[33] Wilson M, Lagowski J, Jastrzebski L, Savtchouk A, Faifer V, Seiler DG, Smith PJ, Diebold AC, McDonald R, Bullis WM, Shaffner TJ, Secula EM. COCOS (corona oxide characterization of semiconductor) non-contact metrology for gate dielectrics. *AIP Conference Proceedings* 2001;550:220-225.
[34] Rein S, Glunz SW. Electronic properties of interstitial iron and iron-boron pairs determined by means of advanced lifetime spectroscopy. *J Appl Phys* 2005;98:113711.
[35] Heiser T, Weber ER. Transient ion-drift-induced capacitance signals in semiconductors. *Phys Rev B* 1998;58:3893-3903.
[36] Heiser T, Belayachi A, Schunck JP. Copper Behavior in Bulk Silicon and Associated Characterization Techniques. *Journal of The Electrochemical Society* 2003;150:G831-G837.
[37] Lindroos J, Savin H. Review of light-induced degradation in crystalline silicon solar cells. *Sol Energ Mat Sol Cells* 2016;147:115-126.
[38] Koveshnikov S, Pan Y, Mollenkopf H. *Proceedings of the Fourth International Symposium on High Purity Silicon,* San Antonio, Texas, USA, 6-11 October 1996, (The Electrochemical Society, Pennington, NJ, USA, 1996), p. 473.
[39] Weber ER. Transition metals in silicon. *Appl Phys A* 1983;30:1-22.